SCIENCE CHINA
Life Sciences

•COVER ARTICLE•

July 2022 Vol.65 No.7: 1271–1284
https://doi.org/10.1007/s11427-022-2122-0

A neuropsin-based optogenetic tool for precise control of G_q signaling

Ruicheng Dai[2,3,7†], Tao Yu[1,2,7†], Danwei Weng[4,2†], Heng Li[1,2,6], Yuting Cui[2], Zhaofa Wu[8,9], Qingchun Guo[10,5], Haiyue Zou[11,5], Wenting Wu[1,2,7], Xinwei Gao[5], Zhongyang Qi[2], Yuqi Ren[2], Shu Wang[5], Yulong Li[8,9] & Minmin Luo[2,4,5,6*]

[1]*School of Life Sciences, Tsinghua University, Beijing 100084, China;*
[2]*National Institute of Biological Sciences (NIBS), Beijing 102206, China;*
[3]*School of Life Sciences, Peking University, Beijing 100871, China;*
[4]*Graduate School of Peking Union Medical College, Beijing 100730, China;*
[5]*Chinese Institute for Brain Research, Beijing 102206, China;*
[6]*Tsinghua Institute of Multidisciplinary Biomedical Research (TIMBR), Beijing 102206, China;*
[7]*Peking University-Tsinghua University-NIBS Joint Graduate Program, NIBS, Beijing 102206, China;*
[8]*State Key Laboratory of Membrane Biology, Peking University School of Life Sciences, Beijing 100871, China;*
[9]*PKU-McGovern Institute for Brain Research, Beijing 100871, China;*
[10]*Capital Medical University, Beijing 102206, China;*
[11]*Academy for Advanced Interdisciplinary Studies, Peking University, Beijing 100871, China*

Received April 12, 2022; accepted April 29, 2022; published online May 12, 2022

G_q-coupled receptors regulate numerous physiological processes by activating enzymes and inducing intracellular Ca^{2+} signals. There is a strong need for an optogenetic tool that enables powerful experimental control over G_q signaling. Here, we present chicken opsin 5 (cOpn5) as the long sought-after, single-component optogenetic tool that mediates ultra-sensitive optical control of intracellular G_q signaling with high temporal and spatial resolution. Expressing cOpn5 in HEK 293T cells and primary mouse astrocytes enables blue light-triggered, G_q-dependent Ca^{2+} release from intracellular stores and protein kinase C activation. Strong Ca^{2+} transients were evoked by brief light pulses of merely 10 ms duration and at 3 orders lower light intensity of that for common optogenetic tools. Photostimulation of cOpn5-expressing cells at the subcellular and single-cell levels generated fast intracellular Ca^{2+} transition, thus demonstrating the high spatial precision of cOpn5 optogenetics. The cOpn5-mediated optogenetics could also be applied to activate neurons and control animal behavior in a circuit-dependent manner. cOpn5 optogenetics may find broad applications in studying the mechanisms and functional relevance of G_q signaling in both non-excitable cells and excitable cells in all major organ systems.

chicken opsin 5, astrocytes, photostimulation, Ca^{2+} imaging, IP3, protein kinase C, neural circuit

Citation: Dai, R., Yu, T., Weng, D., Li, H., Cui, Y., Wu, Z., Guo, Q., Zou, H., Wu, W., Gao, X., et al. (2022). A neuropsin-based optogenetic tool for precise control of G_q signaling. Sci China Life Sci 65, 1271–1284. https://doi.org/10.1007/s11427-022-2122-0

INTRODUCTION

G-protein-coupled receptors (GPCRs) modulate many intracellular signaling pathways and represent some of the most intensively studied drug targets (Hauser et al., 2017). Upon ligand binding, the GPCR undergoes a conformation change that is transmitted to heterotrimeric G proteins, which are multi-subunit complexes comprising G_α ($G_{q/11}$, G_s, $G_{i/o}$

†Contributed equally to this work
*Corresponding author (email: luominmin@cibr.ac.cn)

and $G_{12/13}$) and tightly associated $G_{\beta\gamma}$ subunits (Wettschureck and Offermanns, 2005). The G_q proteins, a subfamily of G_α subunits, couple to a class of GPCRs to mediate cellular responses to neurotransmitters, sensory stimuli, and hormones throughout the body (Exton, 1996; Ritter and Hall, 2009). Their primary downstream signaling targets include phospholipase C beta (PLC-β) enzymes, which catalyze the hydrolysis of phospholipid phosphatidylinositol bisphosphate (PIP_2) into inositol trisphosphate (IP_3) and diacylglycerol (DAG). IP_3 triggers intracellular Ca^{2+} release, which together with DAG activates protein kinase C (PKC) (Kadamur and Ross, 2013). The activation of G_q-coupled receptors often produces rapid (within seconds) and robust increase in Ca^{2+} signals (Clapham, 2007). Given that Ca^{2+} signals and PKC activity impact nearly every cellular process, developing tools that precisely control intracellular G_q signaling would be highly valuable for studying the mechanisms and physiological functions of G_q-coupled receptors.

Optogenetics uses light-responsive proteins to achieve optically-controlled perturbation of cellular activities with genetic specificity and high spatiotemporal precision (Boyden et al., 2005; Fenno et al., 2011). Since the early discoveries of optogenetic tools using light-sensitive ion channels and transporters, diverse technologies have been developed and now support optical interventions into intracellular second messengers, gene transcription, and protein interactions and degradation (Lu et al., 2020; Quadrato et al., 2017; Rost et al., 2017; Tye and Deisseroth, 2012; Zhang et al., 2011). Optogenetic tools that control G_q signaling may have several advantages over current approaches, including chemogenetics and photoactivatable small molecules (Adams and Tsien, 1993; Gomez et al., 2017; Herlitze and Landmesser, 2007): unlike chemogenetics, they potentially offer subsecond temporal resolution and subcellular spatial resolution; unlike photoactivatable compounds, they provide control of genetically-identified cell types in complex organ systems. However, despite several intensive efforts, to date, there has been few optogenetic tools that enable rapid and effective activation of G_q signaling (Spoida et al., 2014; Spoida et al., 2016; Vaezy et al., 2001). Opto-a1AR, a creatively designed G_q-coupled rhodopsin-GPCR chimera, induces mild intracellular Ca^{2+} increase only after long-time (>60 s) photostimulation (Airan et al., 2009). Melanopsin (Opn4) in a subset of mammalian retinal ganglion cells is a G_q-coupled opsin that mediates no-image-forming visual functions (Güler et al., 2008; Hankins et al., 2008; Hattar et al., 2002; Panda et al., 2003; Xue et al., 2011). However, cells expressing Opn4 isoforms show weak Ca^{2+} responses even after prolonged (15–60 s) exposure to bright light illumination, and require continuous chromophore addition in the culture medium (Melyan et al., 2005; Mure et al., 2016; Qiu et al., 2005). Indeed, systematic characterizations have revealed major limitations of these two tools for *in vitro* and *in vivo* applications (Figueiredo et al., 2014; Gerasimov et al., 2021; Mederos et al., 2019). Opto-a1AR and Opn4 thus only partially mimic the activation of endogenous G_q-coupled receptors.

We asked whether some naturally occurring photoreceptors could serve as efficient optogenetic tools for G_q signaling. Most animals detect light using GPCR-based photoreceptors, which comprise a protein moiety (opsin) and a vitamin A derivative (retinal) that functions as both a ligand and a chromophore (Terakita, 2005). Several thousand opsins have been identified to date (Koyanagi and Terakita, 2014; Yau and Hardie, 2009), and two recent studies reported G_i-based opsins from mosquito and lamprey for presynaptic inhibition in neurons (Copits et al., 2021; Mahn et al., 2021). Opn5 (neuropsin) and its orthologs in many vertebrates have been reported as ultraviolet (UV)-sensitive opsins that couple to G_i proteins (Calligaro et al., 2022; Kojima et al., 2011; Yamashita et al., 2010; Zhang et al., 2020). Interestingly, exposure to blue light induces an increase in intracellular Ca^{2+} levels within avian primary Müller glial cells endogenously expressing Opn5 (Rios et al., 2019), hinting the possibility that certain Opn5 might also couple to G_q proteins (Nakane et al., 2010; Nakane et al., 2014).

Here we report that the chicken Opn5 (cOpn5 for simplicity), but not two of its mammalian orthologs, sensitively and strongly mediated blue light-induced activation of G_q signaling in mammalian cells. Detailed characterizations of cOpn5 reveal that it is at least 3 orders of magnitude higher in light sensitivity and temporal precision than existing G_q-coupled opsin-based tools, opto-a1AR and Opn4. cOpn5 provides subcellular spatial resolution and does not require chromophore addition. We further demonstrate cOpn5 optogenetics as a highly effective approach for activating neurons to produce robust behavior changes in freely moving mice. These findings establish that cOpn5 can be utilized as powerful, single-component optogenetic tools to support experimental investigations into the mechanisms and functions associated with G_q signaling.

RESULTS

cOpn5-mediated optogenetics activates G_q signaling

We tested whether heterologous expression of the Opn5 orthologs from chicken, humans, and mice (which share 80%–90% protein sequence identity, Tables S1 and S2 in Supporting Information) have the capacity to mediate blue light-induced G_q signaling activation within HEK 293T cells (Figure 1A). The cOpn5 was co-localized with the EGFP-CAAX membrane maker, indicating that it was effectively expressed on the plasma membrane (Figure 1B; Table S3 in Supporting Information listed the primers for recombinant

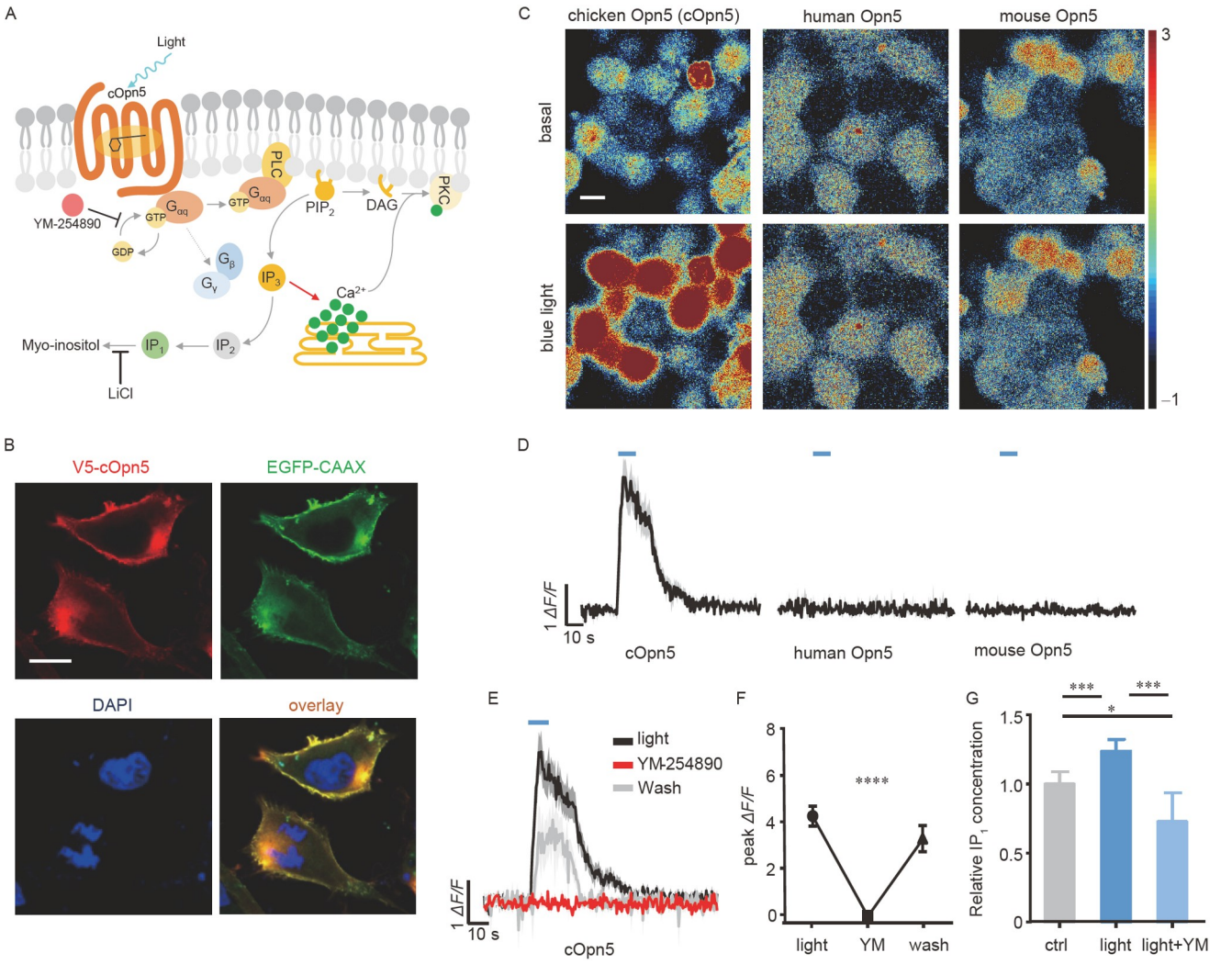

Figure 1 cOpn5 mediates optical activation of G_q signaling in HEK 293T cells. A, Schematic diagram shows the putative intracellular signaling in response to light-induced cOpn5 activation. PLC: phospholipase C; PIP_2: phosphatidylinositol-4,5-bisphosphate; IP_3: inositol-1,4,5-trisphosphate; IP_1: inositol monophosphate; YM-254890: a selective G_q protein inhibitor. B, The Cy3-counterstained V5-cOpn5 fusion protein (red) was co-localized with the membrane-tagged EGFP-CAAX (green) in HEK 293T cells. DAPI counterstaining (blue) indicates cell nuclei. Scale bar, 10 μm. C, Pseudocolor representation of the Ca^{2+} signals before and after blue light stimulation (10 s; 100 μW mm^{-2}; 488 nm) in HEK 293T cells expressing Opn5 from three species (*Gallus gallus*, *Homo sapiens*, and *Mus musculus*). Scale bar, 10 μm. D, Time courses of light-evoked Ca^{2+} signals for cells shown in (C). Blue lines above the curves indicate light stimulation. Ca^{2+} indicator fluorescence intensity relative to its resting fluorescence intensity; abbreviated as $\Delta F/F$. E, The G_q protein inhibitor YM-254890 (10 nmol L^{-1}) reversibly blocked cOpn5-mediated, light-induced Ca^{2+} signals (n=28 HEK 293T cells). We used 10 min wash time to observe the reversal of drug effect. F, Group data show that the G_q protein inhibitor YM-254890 (10 nmol L^{-1}) reversibly blocked cOpn5-mediated, light-induced Ca^{2+} signals (n=28 HEK 293T cells). ****, P<0.0001, one way ANOVA. Error bars indicate SEM. G, YM suppressed the IP_1 accumulation evoked by continuous light stimulation (3 min; 100 μW mm^{-2}; 470 nm) in cOpn5-expressing HEK 293T cells (n=4 replications). *, P=0.0108, ***, P<0.001, unpaired t-tests. Ctrl indicates cOpn5-expressing cells without light or drug application.

plasmids). We used blue light for stimulation and the red intracellular Ca^{2+} indicator Calbryte™ 630 AM dye to monitor the relative Ca^{2+} response (Figure 1C; Table S4 in Supporting Information listed the light resources). cOpn5 mediated an immediate and strong light-induced increase in Ca^{2+} signal (~3-fold increase in Ca^{2+} indicator fluorescence intensity relative to its resting fluorescence intensity; abbreviated as $\Delta F/F$), whereas no light effect was observed from cells expressing the human or mouse Opn5 orthologs (Figure 1D; Video 1 in Supporting Information). Note that we did not supply any exogenous retinal to the culture media, which suggested that the low-level endogenous retinal is sufficient to render cOpn5 functional (Brueggemann and Sullivan, 2002). Thus, unlike mammalian Opn5, cOpn5 allows effective optical activation of intracellular Ca^{2+} signals in the human HEK 293T cells.

We then examined whether cOpn5 truly mediated the activation of G_q signaling, which triggers signal cascades that produce two second messengers: IP_3 leading to Ca^{2+} releases from intracellular stores, and DAG leading to PKC activation. Preincubation of YM-254890, a highly selective G_q proteins inhibitor (Taniguchi et al., 2003), reversibly abol-

ished the light-induced Ca^{2+} transients in cOpn5-expressing cells (Figure 1E and F). We observed strong Ca^{2+} signals in the absence of extracellular Ca^{2+}, thus indicating Ca^{2+} release from intracellular stores (Figure S1A in Supporting Information). In cOpn5-, but not human OPN5-expressing cells, we also detected a light-induced increase in the level of inositol phosphate (IP_1), the rapid degradation product of IP_3; moreover, the extent of this increase was reduced with the treatment of YM-254890 (Figure 1G; Figure S1D in Supporting Information; Table S5 in Supporting Information listed the detailed information of statistical analyses). This result thus indicated light-evoked, G_q-dependent IP_3 production. In cOpn5-expressing HEK 293T cells, blue light also triggered the phosphorylation of MARCKS protein, a well-known target of PKC (Hartwig et al., 1992), in a PKC activity-dependent manner (Figure S1B and C in Supporting Information). Consistent with earlier findings indicating that mammalian Opn5 couples to G_i (Kojima et al., 2011; Yamashita et al., 2010; Zhang et al., 2020), blue light illumination effectively reduced cAMP levels in cells expressing human and mouse Opn5 with additional retinal; however, it had very mild effect in cOpn5-expressing cells in the presence of retinal and had no effect without retinal (Figure S1E in Supporting Information). Collectively, these data revealed that blue light illumination enables the efficient coupling of cOpn5, but not its mammalian orthologs, to the G_q signaling pathway in mammalian cells.

cOpn5-mediated optogenetics is sensitive and precise

Given that light-stimulated cOpn5 mimics endogenous G_q-coupled GPCRs to rapidly activate the G_q signaling pathway, we asked whether cOpn5 could serve as the long sought-after optogenetic tool for G_q signaling, and more importantly, whether it has features common to other popular optogenetic tools, such as high light sensitivity, single-component convenience, and high spatiotemporal resolution. We first systematically characterized the light-activating properties of cOpn5-expressing HEK 293T cells. Although Opn5 is previously considered as an ultraviolet (UV)-sensitive photoreceptor (Yamashita et al., 2010), mapping with a set of wavelengths ranging 365–630 nm at a fixed light intensity of (100 μW mm^{-2}) revealed that the 470 nm blue light elicited the strongest Ca^{2+} transients, with the UVA light (365 and 395 nm) being less effective and longer-wavelength visible light (561 nm or above) completely ineffective (Figure 2A). We then tested the effects of varying photostimulation durations. Stimulating with brief light pulses (1, 5, 10, 20, 50 ms; 16 μW mm^{-2}; 470 nm) showed that the Ca^{2+} response achieved the saturation mode with light duration over 10 ms. Longer light durations did not further increase the Ca^{2+} signal amplitude at this light intensity (Figure 2B). Delivering brief blue light pulses (10 ms; 470 nm) at different intensities showed that the light of ~4.8 and 16 μW mm^{-2} produced about half maximum and full maximum responses, respectively (Figure 2C; Figure S2D in Supporting Information). The response time courses revealed that 10 ms blue light pulses (16 μW mm^{-2}) generated significant Ca^{2+} signals within 1 s and produced peak responses within 2.5 s (time to 10% peak activation=(1.36±0.55) s; time to 90% peak activation=(2.37±0.87) s, decay time τ=(18.66±4.98) s; Figure 2C; Figure S2D in Supporting Information). Therefore, the light sensitivity of cOpn5 is 3–4 orders of magnitude higher than the reported values of the light-sensitive G_q-coupled GPCRs and even 2–3 orders higher than those of the commonly used optogenetic tool Channelrhodopsin-2 (ChR2) (Lin, 2011; Zhang et al., 2006) (Table S6 in Supporting Information listed the comparison cOpn5 with other optogenetic tools). Together, these results indicate that cOpn5 could function as a single-component optogenetic tool without additional retinal, and that cOpn5 is supersensitive to blue light for its full activation requiring low light intensity (16 μW mm^{-2}) and short duration (10 ms).

Designer Receptors Exclusively Activated by Designer Drugs (DREADD)-based chemogenetic tools efficiently modulate cellular activity (Roth, 2016; Urban and Roth, 2015). For example, hM3Dq expression allows the activation of G_q signaling by adding the exogenous small molecule ligand clozapine-N-oxide (CNO) (Gomez et al., 2017; Krashes et al., 2011; Rogan and Roth, 2011). We thus compared the Ca^{2+} signals in response to 10 s infusion of CNO on hM3Dq-expressing HEK 293T cells to that evoked by 10 s photostimulation of cOpn5-expressing cells. Although the response amplitudes were similar, cOpn5-mediated optogenetic stimulation produced faster and temporally more precise response, as well as more rapid recovery than hM3Dq-mediated chemogenetic stimulation (Figure 2B; Figure S2A–C in Supporting Information). These results thus indicate that cOpn5-mediated optogenetics is more controllable in temporal accuracy than those of hM3Dq-mediated chemogenetics.

cOpn5 optogenetics also provides the major advantage of spatially precise control of cellular activity. Restricting brief light stimulation (63 ms) into individual cOpn5-expressing HEK 293T cells resulted in the immediate activation of the stimulated cell. Interestingly, in high cell confluence areas, the Ca^{2+} signals propagated to surrounding cells, thus suggesting intercellular communication among HEK 293T cells through a yet-to-identified mechanism (Figure 2D and E; Video 2 in Supporting Information).

We directly compared the performance of cOpn5 to those of opto-a1AR and Opn4, which had been proposed for optogenetic control of G_q signaling. Following the protocol in a previous report (Airan et al., 2009), we found that 15 s illumination at the rather strong intensity level (7 mW mm^{-2}) was completely ineffective in opto-a1AR-epxpressing cells; further increasing the light exposure duration to 60 s trig-

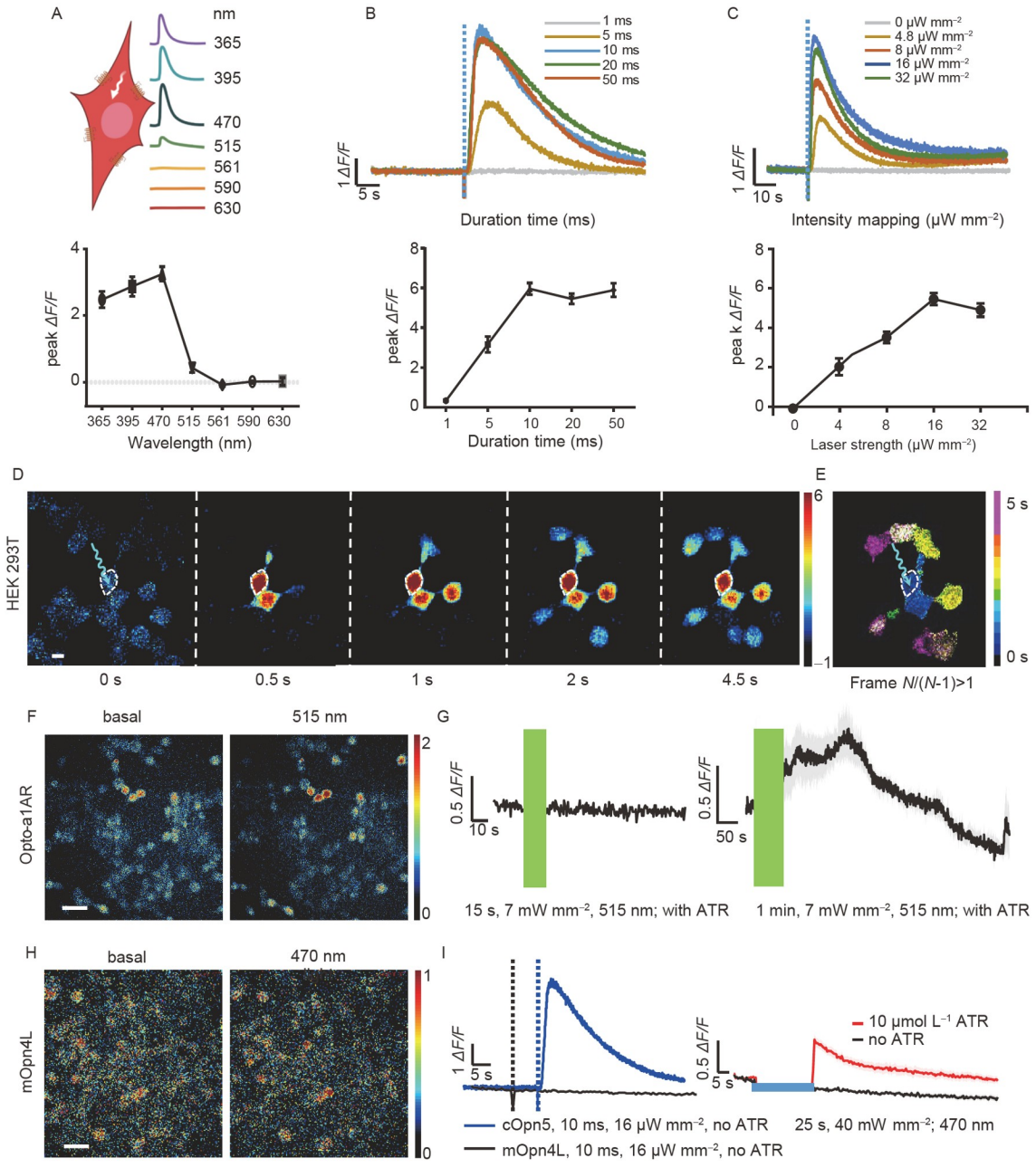

Figure 2 cOpn5 sensitively mediates optical control of G_q signaling with high temporal and spatial resolution. A, Schematic diagram of selected wavelengths (365, 395, 470, 515, 561, 590, and 630 nm) and the raw traces of Ca^{2+} signals (top panel) and the mean amplitudes of Ca^{2+} signal of cOpn5-expressing HEK 293T cells in response to light stimulation with different wavelengths (2 s; 100 μW mm^{-2}; bottom panel). Error bars indicate SEM. B, Time course of Ca^{2+} signals evoked by cOpn5-mediated optical activation using light pulses of different durations (1, 5, 10, 20, or 50 ms; 16 μW mm^{-2}; 470 nm; n=49 HEK 293T cells) (top panel) an the mean response magnitudes to light stimulation of different durations (1, 5, 10, 20, or 50 ms; 16 μW mm^{-2}; 470 nm) (bottom panel). Error bars indicate SEM. C, Time course of cOpn5-mediated Ca^{2+} signals under different light intensity (0, 4.8, 8, 16, or 32 μW mm^{-2}; 10 ms; 470 nm, mean±SEM.; n=10 cells) (top panel) and the mean response magnitude under different light intensities (0, 4.8, 8, 16, or 32 μW mm^{-2}) at 10 ms, 470 nm (n=88 HEK 293T cells) (bottom panel). Error bars indicate SEM. For 10 ms, 16 μW mm^{-2} stimulation, time to 10% peak activation=(1.36±0.55) s; time to 90% peak activation=(2.37±0.87) s; decay time τ=(18.66±4.98) s. D, Images of light-induced (63 ms;17 μW; arrow points to the stimulation region) Ca^{2+} signal propagation from the stimulated HEK 293T cell to surrounding cells. Scale bar, 10 μm. E, Pseudocolor images showing the process of Ca^{2+} signal propagation across time of (D) (frame N/(N−1)>1). Frame interval was 500 ms and each frame is counted once. F, Pseudocolor images of the baseline and peak Ca^{2+} signals ($\Delta F/F0$) in opto-a1AR-expressing HEK 293T cells. The medium buffer contains 10 μmol L^{-1} ATR. Scale bar, 30 μm. G, The lack of effect by 15 s light stimulation on Ca^{2+} signals (left panel) and mild effect of 60 s light stimulation on the Ca^{2+} in opto-a1AR-expressing HEK 293T cells (right panel; n=15 cells). Green bars indicate light stimulations. H, Pseudocolor images of the baseline and peak Ca^{2+} signals ($\Delta F/F0$) in mOpn4L-expressing HEK 293T cells. The medium buffer contains 10 μmol L^{-1} all-trans-retinal. Scale bar, 30 μm. I, The left panel shows that without ATR, brief light pulses (10 ms, 16 μW mm^{-2}, 470 nm) evoked strong Ca^{2+} signals in cOpn5-expressing cells (blue line; n=10 HEK 293T cells) but had no effect on mOpn4L-expressing cells (black line; n=12 HEK 293T cells). The right panel shows the effect of 25 s, 40 mW mm^{-2} light stimulation on the Ca^{2+} in mOpn4L-expressing HEK 293T cells within 10 μmol L^{-1} ATR (n=12 cells; red line) and the lack of such effect following ATR removal (black line). Two dashed lines indicate light stimulation and blue bar indicates 25 s light stimulation.

gered a slow and small (~0.5 $\Delta F/F$) Ca^{2+} signal increase (Figure 2F and G). We also compared the performance of cOpn5 to that of mouse Opn4L (mOpn4L), a natural opsin which was reported as a tool for G_q signaling activation (Panda et al., 2005; Qiu et al., 2005). Without the addition of all-trans-retinal (ATR), neither brief blue light pulses (16 μW mm^{-2}) nor prolonged strong light illumination (25 s, 40 mW mm^{-2}, 470 nm) had slightly effect on the Ca^{2+} signals in mOpn4L-expressing HEK 293T cells (Figure 2H and I). Following the addition of exogenous ATR, long exposure of very strong illumination (25 s; 40 mW mm^{-2}) triggered a slow Ca^{2+} signal increase (~1 $\Delta F/F$) in mOpn4L-expressing cells; by contrast, in cOpn5-expressing cells the light pulses of only 1/2,500 duration (10 ms) and 1/2,500 intensity (16 μW/mm^2) produced nearly 6-fold increase in Ca^{2+} signals (Figure 2H and I). Therefore, compared with existing opsin-based tools (opto-a1AR and mOpn4L), cOpn5 is much more light-sensitive (at least ~3 orders higher sensitivity), requires much shorter time exposure (10 ms *vs*. 25 s or 60 s), and produces severalfold stronger responses (Table S6 in Supporting Information).

cOpn5-mediated optogenetics effectively activates primary astrocytes and neurons

Astrocytes represent an important population of non-excitable cells in the central nervous system and are known to regulate a variety of processes, including neurogenesis and synaptogenesis, blood-brain barrier permeability, and extracellular homeostasis (Abbott et al., 2006; Allen and Eroglu, 2017; Linnerbauer et al., 2020; Sofroniew, 2015; Zonta et al., 2003). However, to date, direct optogenetic control of astrocytes has achieved only limited success (Xie et al., 2015; Yu et al., 2020). We expressed cOpn5 in primary astrocyte cultures prepared from the neonatal mouse brain with AAV vectors for bicistronic expression of cOpn5 and the EGFP marker protein (Figure S3 in Supporting Information). Using the Calbryte™ 630 AM dye to monitor Ca^{2+} levels, we found that blue light illumination of cOpn5-expressing astrocytes produced strong Ca^{2+} transients (~8 $\Delta F/F$), which were also reversibly blocked by the G_q inhibitor YM-254890 (Figure 3A–C; Video 1 in Supporting Information).

We explored the application of cOpn5-mediated optogenetics directly in neurons. We first examined whether cOpn5 could mediate light-induced Ca^{2+} signals. Using AAV and the pan-neuronal SYN promoter, we expressed cOpn5 and the red Ca^{2+} indicator jRGECO1a in mouse cortical neurons (Figure 4A). In brain slice preparations, application of blue light pulses (10 s; 100 μW mm^{-2}; 473 nm) reliably evoked Ca^{2+} transients in neurons (Figure 4B and C). Thus, cOpn5 also enables light-induced activation in neurons.

We investigated the effect of light-induced cOpn5 activation on the electrophysiological properties of neurons in slice preparations (Figure 4D) (Luo, 2020). We observed two types of activation patterns of cortical and subcortical neurons. In a majority of neurons (17 out 29 neurons), brief light pulses (10 ms) rapidly evoked strong inward currents (100–1,000 pA) and drove vigorous firing of action potentials (Figure 4E (left) and F). In the other 12 out of the 29 neurons recorded, blue light pulses (10 ms) induced a small depolarizing current (~20 pA) in the voltage-clamp mode, and induced delayed-yet-robust firing of action potentials in the current-clamp mode (Figure 4E (right) and F). Neurons were repeatedly stimulated with 10 ms pulses at 10 Hz, and exhibited a non-attenuated mode in firing rate across repetitive trials of light stimulation (Figure 4G). Of note, unlike those generated by ChR2 optogenetics (Tian et al., 2009), the action potentials evoked by cOpn5 photostimulation were not time-locked to light pulses in any of neurons recorded.

cOpn5-mediated optogenetics controls animal behaviors

We assessed the utility of cOpn5-mediated optogenetics for

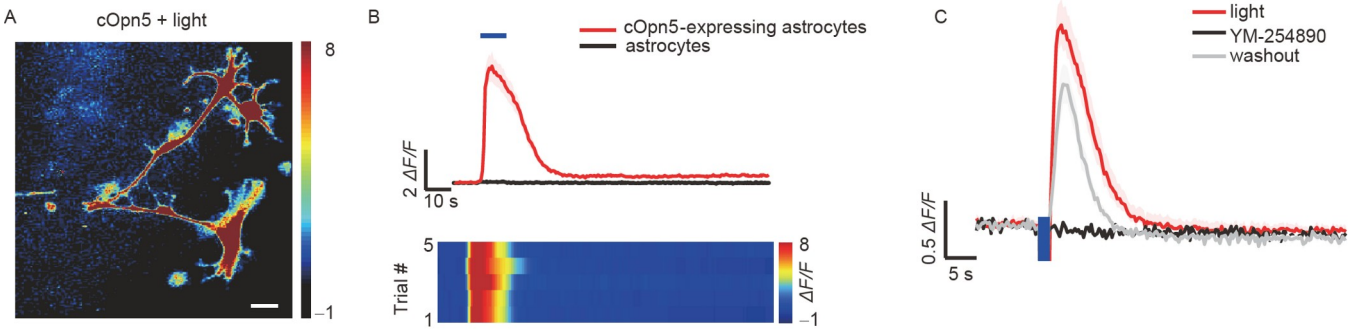

Figure 3 cOpn5 optogenetics effectively activates astrocytes. A, Pseudocolor images of the baseline and peak Ca^{2+} signals following light stimulation of cOpn5-expressing astrocytes. Scale bar, 20 μm. B, Plot of Ca^{2+} signals and heat map representation of Ca^{2+} signals across trials (n=25 astrocytes). C, Group data show that the G_q protein inhibitor YM-254890 (30 nmol L^{-1}) reversibly blocked cOpn5-mediated, light-induced Ca^{2+} signals of cOpn5-expressing astrocytes (n=20 astrocytes). P<0.0001 for difference between light and YM, one way ANOVA. Blue bar indicates 1 s light stimulation. Light stimulation interference was cleaved for clarity.

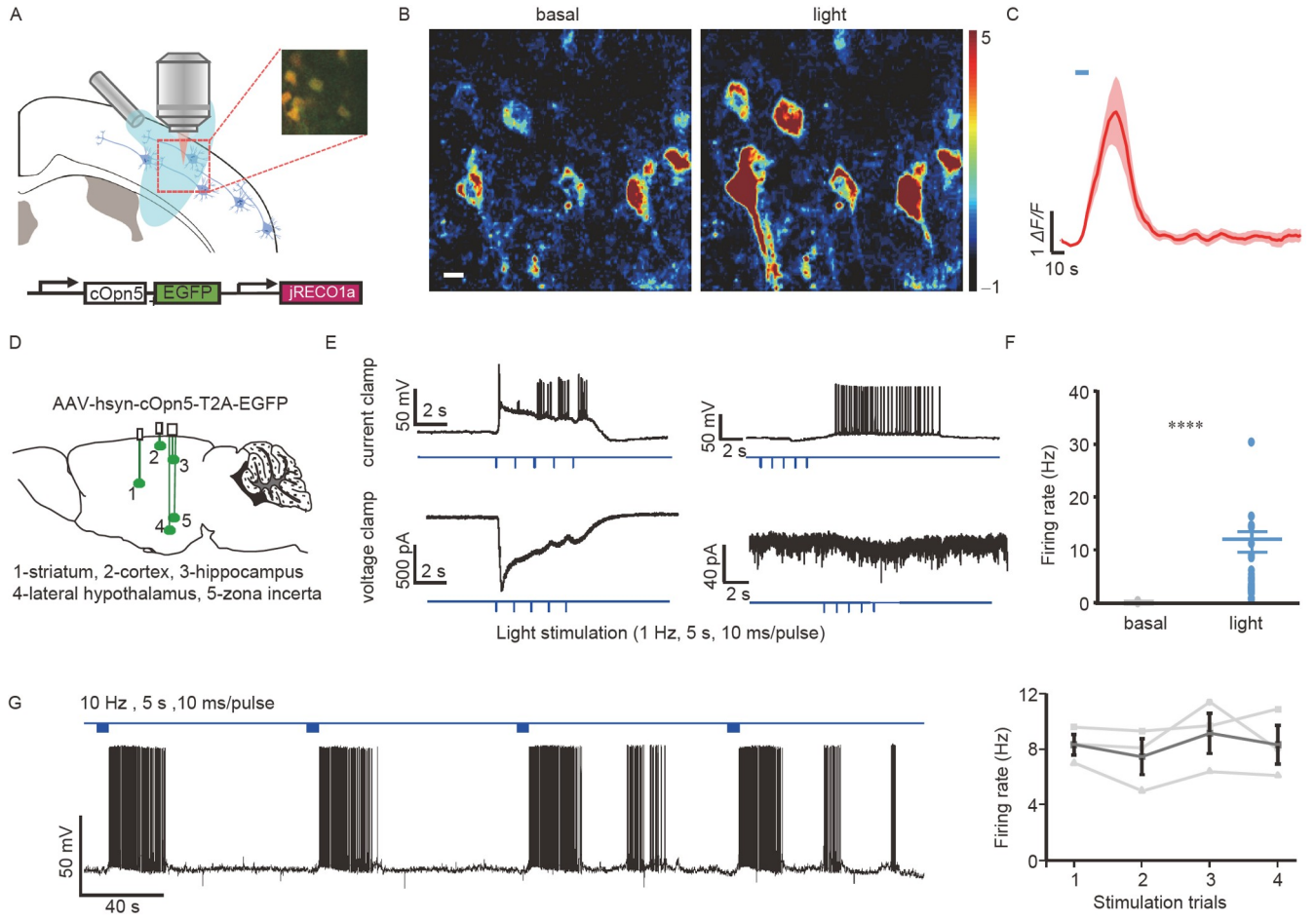

Figure 4 cOpn5-mediated optogenetics activation of neurons. A, Schematic diagram shows the experimental setup for optogenetic stimulation and Ca^{2+} imaging. We used AAV vectors to express cOpn5, EGFP, and the red Ca^{2+} sensor jRECO1a in neurons. The raw image shows the expression of EGFP and jRECO1a within the same set of neurons. B, Pseudocolor images show Ca^{2+} signals before and after light stimulation (10 s; 100 μW mm^{-2}; 473 nm). Scale bar, 10 μm. C, Group data of Ca^{2+} signal traces of 6 individual neurons shown in (B). D, Schematic diagram depicts optogenetic stimulation and whole-cell patch-clamp recording of cOpn5-expressing neurons in the cortex, striatum, hippocampus, lateral hypothalamus (LH), and zonal incerta (ZI). E, Raw data illustrate two representative patterns of light-evoked neuronal activation. One neuron (left panels) exhibited rapid membrane potential depolarization and large inward currents (1 Hz,5 s, 10 ms/pulse), and another neuron (right panels) exhibited strong, delayed firing of action potentials yet small sustained inward currents in response to the light pulses. F, Group data show the neuronal firing rates before and after pulsed 473 nm light stimulation (20 Hz, 1 s; n=29 neurons; ****, P<0.0001, unpaired t-test). G, Raw trace shows that cOpn5 mediated reliable and reproducible photoactivation of a neuron (left). The right panel shows the summary of firing rates across repetitive trials of light stimulation (n=3 neurons).

modulating animal behavior. The lateral hypothalamus (LH) participates in reward processing and feeding regulation (Jennings et al., 2013; Li et al., 2018; Stuber and Wise, 2016). We expressed cOpn5 in the LH GABAergic neurons of *VGAT*-Cre mice and implanted optical fibers to deliver light pulses into the LH of freely behaving mice (Figure 5A; Figure S4A in Supporting Information). Consistent with a role of LH GABA neurons in promoting feeding behavior (Li et al., 2018), light stimulation (20 Hz; 5 ms/pulse; 473 nm; 0.75 mW output from the fiber tip) elicited a significant increase in food intake in cOpn5-expressing mice but not the EGFP-expressing control mice (Figure 5B). We also used a food-foraging behavior task to test the effect of cOpn5-mediated optogenetic activation of GABA neurons in the zona incerta (ZI) (Figure 5C; Figure S4B in Supporting Information), a region known to drive compulsive eating (Zhang and van den Pol, 2017). cOpn5-expressing mice, but not the EGFP-expressing mice, showed a significantly increase in the time of foraging high-fat food pellets upon repeated light stimulation (Figure 5D). Notably, mice maintained the behavior (feeding behavior or high-fat food foraging behavior) while the light was on, and immediately stopped the behavior when the light was off (Video 3 in Supporting Information). Confirming the validity of optogenetic activation, blue light pulses rapidly elicited vigorous firing of action potentials from cOpn5-expressing neurons within the LH and ZI (Figure 5E and F). Thus, cOpn5 is effective for rapidly, accurately, and reversibly activating neurons and controlling animal behavioral states.

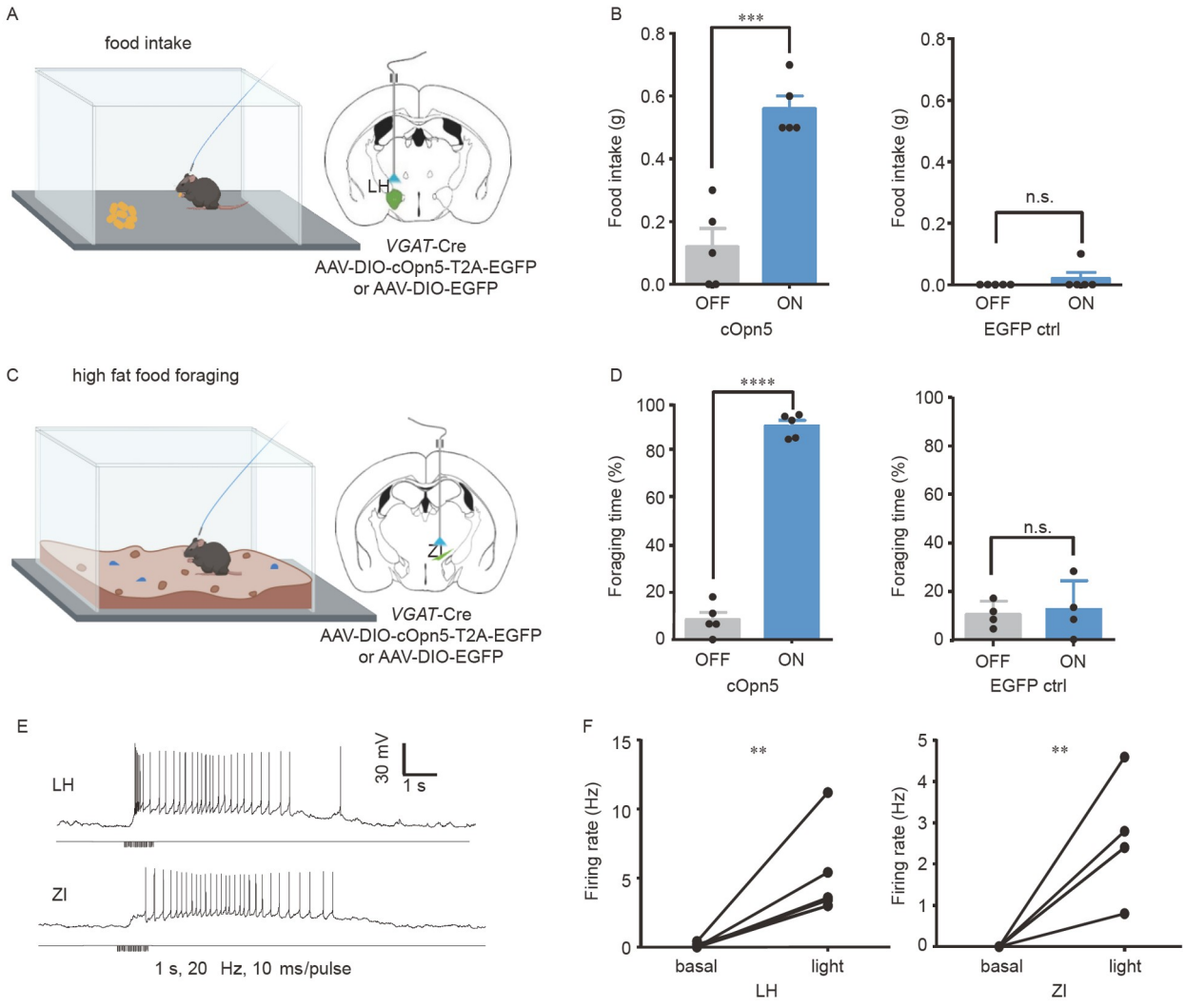

Figure 5 cOpn5-mediated optogenetics activation changes the mouse behaviors in a neural circuit-dependent manner. A, Schematic diagram of the experimental setup for cOpn5 optogenetics and food intake assay. cOpn5 and EGFP were expressed in GABAergic neurons within the LH of *VGAT*-Cre mice. EGFP was expressed as a control. B, Summary data show the light-induced (20 Hz; 5 ms/pulse; 473 nm; 0.75 mW output from the fiber tip), cOpn5-mediated activation of eating behaviors. ***, P=0.0003; n.s., non-significant; n=6 mice; unpaired t-test. Error bars indicate SEM. C, Schematic diagram of the experimental setup for food foraging behavior. High-fat food pellets were used. cOpn5 and EGFP were expressed in GABAergic neurons within the ZI of *VGAT*-Cre mice. EGFP was expressed as a control. D, Summary data show the cOpn5-mediaed food foraging behaviors. Foraging time percentage was calculated upon receiving light stimulation until the mouse found the hidden food. ****, P<0.0001; n=6 mice; unpaired t-test. Error bars indicate SEM. E, Raw data illustrate the pattern of cOpn5-mediated optical activation of GABAergic neurons in these two brain areas. F, Group data show the neuronal firing rates before and after pulsed 473 nm light stimulation (1 Hz, 5 s; for the LH, n=6 neurons, **, P=0.0041, unpaired t-tests; for the ZI, n=5 neurons, **, P=0.0027, unpaired t-tests).

DISCUSSION

Here, we demonstrate the use of cOpn5 as an extremely effective optogenetic tool for activating G_q signaling. Previous studies have characterized mammalian Opn5 as a UV-sensitive G_i-coupled opsin; we present the surprising finding that visible blue light can induce rapid Ca^{2+} transients, IP_1 accumulation, and PKC activation in cOpn5-expressing mammalian cells. We show that cOpn5 allows optical activation of neurons and precise control of animal behaviors. Importantly, cOpn5 is a powerful yet easy-to-use, single-component system that does not require an exogenous chromophore. We envision that cOpn5-based optogenetics will be an enabling technique for investigating the important physiological and behavioral functions regulated by G_q signaling.

Table S6 in Supporting Information lists the key features of cOpn5 by directly comparing its response amplitudes, light sensitivity, temporal resolution, and the requirement of additional chromophores to those of other optogenetic tools. For cOpn5-expressing cells, merely 10 ms blue light pulses at the intensity of 16 μW mm^{-2} evoke rapid increase in Ca^{2+} signals with the peak amplitudes of 3–8 $\Delta F/F$. By contrast, prior characterizations and this study show that the activation

of opto-a1AR or mammalian Opn4, the two proposed optogenetic tools for G_q signaling, require ~3-order higher light intensity (7–40 mW mm^{-2}) and prolonged light exposure (20–60 s) but produce only weak Ca^{2+} signals (0.25–1 $\Delta F/F$). Therefore, opto-a1AR or mammalian Opn4 cannot mimic the rapid activation profiles of endogenous G_q-coupled receptors that often trigger strong Ca^{2+} release upon the application of their corresponding ligands. We demonstrate the power of cOpn5 optogenetics by showing the striking physiological and behavioral effects in response to cOpn5-mediated optical activation of neurons *in vivo*. By contrast, recent *ex vivo* studies show that opto-a1AR- and Opn4-mediated optogenetic stimulations slightly increase the amplitudes of Ca^{2+} signals and only mildly modulate the frequency of Ca^{2+} transients and synaptic events even after prolonged illumination (Gerasimov et al., 2021; Mederos et al., 2019). By overcoming the limitations of light sensitivity, temporal resolution, and response amplitudes associated with opto-a1AR- and Opn4-mediated optogenetics, cOpn5 should find broad applicability for studying G_q signaling in numerous cells and tissues.

cOpn5 optogenetics also enjoys the benefits of safety and convenience. Although Opn5 from many species is reported UV-responsive (Kojima et al., 2011), cOpn5 is optimally activated by 470 nm blue light, which penetrates better than UV and avoids UV-associated cellular toxicity. Its ultrasensitivity to light minimizes potential heating artifact, suggesting that it is suitable for even deeper tissue activation using a pulsed laser. cOpn5 is strongly, and repetitively activated by light without the requirement for exogenous chromophore, possibly because cOpn5 is a bistable opsin that covalently binds to endogenous retinal and is thus resistant to photobleaching (Koyanagi and Terakita, 2014; Tsukamoto and Terakita, 2010). By contrast, some studies indicate that the mammalian Opn4 requires the addition of chromophore for continuous activation (Melyan et al., 2005; Qiu et al., 2005). cOpn5 as a single-component system is particularly useful for both *in vitro* and *in vivo* studies as it avoids the burden of delivering a compound into the tissue during the experiment.

cOpn5 optogenetics should be particularly useful for precisely activating intracellular G_q signaling, which subsequently triggers Ca^{2+} release from intracellular stores and activates PKC. cOpn5 optogenetics can also stimulate G_q signaling in neurons and control animal behavior in a circuit-dependent manner. cOpn5 differs from current channel-based optogenetic tools, such as ChR2 and its variants, which translocate cations across the plasma membrane. G_q-coupled GPCRs may affect variable downstream signaling in a receptor- and cell-specific manner (Rosenbaum et al., 2009). Indeed, we observed that the same light illumination parameters produce different activation patterns among neurons. In addition, G_q-coupled receptors might also target other types of G proteins in a cell type- and context-dependent manner. Therefore, we recommend characterizing and confirming the activation profiles, similar to the applications of other optogenetic and chemogenetic tools. cOpn5-mediated optogenetic activation does not generate strictly time-locked action potential firing as precisely as that by ChR2 in neurons. Ion channel-based optogenetic tools would be preferable if temporally precise control of action potential firing is necessary. Nevertheless, cOpn5-mediated asynchronous firing activity may also be advantageous for circuit dissection, since it avoids the potential artefact of massively synchronized neuronal activation.

Following the publication of a preprint version of this manuscript (Dai et al., 2022), a recent study reported that, following the preincubation of 2 μmol L^{-1} all-trans-retinal, human OPN5-expressing HEK 293 cells respond to UV light with an increase in G_q-associated signals (Wagdi et al., 2022). By contrast, our data here and several previous studies establish that the Opn5 orthologs from humans and mice activate G_i signaling under UV and blue light in the presence of additional retinal (Calligaro et al., 2022; Kojima et al., 2011; Yamashita et al., 2010; Zhang et al., 2020) (Figure 1C and D; Figure S1E in Supporting Information). Of note, UV light triggers Ca^{2+} influx in a retinal- and transient receptor potential channel-dependent manner in several human cell types that lack the overexpression of any opsin isoforms (Bellono et al., 2013; Hu et al., 2017), which suggests that caution should be taken while interpreting this response as a potential contribution of exogenously expressed opsin. Regardless of the exact signaling mechanism of human OPN5, our experiments show that the chicken Opn5 has several advantages as an optogenetic tool for controlling G_q signals, as it does not require additional retinal, is activable by visible rather than UV light, and respond with about 10 times higher light sensitivity than that of human OPN5 (Wagdi et al., 2022).

In summary, we present cOpn5 as a blue light-sensitive opsin for rapidly, reversibly, and precisely activating G_q signaling. We also establish cOpn5 as a powerful and easy-to-use optogenetic tool for activating both non-excitable cells and neurons *in vitro* and *in vivo*. Given the ubiquitously important roles of G_q-coupled GPCRs, we expect that cOpn5 will be useful for studying the mechanisms and functions of G_q signaling in all major cell types and tissues.

MATERIALS AND METHODS

Mice

Animal care and use conformed to the institutional guidelines of the National Institute of Biological Sciences, Beijing as well as the governmental regulations of China. Male C57BL/6N mice were purchased from Beijing Vital River Laboratory Animal Technology Co., Ltd (China). Adult (8–

16 weeks old) *VGAT*-Cre mice [STOCK Tg(*Slc32a1*-cre) 2.1Hzo/FrkJ] of either sex were obtained from the Jackson Laboratory (USA). All mice were maintained with a 12/12 light/dark cycle (lights off at 8 PM) and housed in groups of five for 6–8 weeks. After surgery, mice were housed in groups with an inverted light-dark cycle (lights off at 8 AM) for at least one week before further experiments. Adult mice of either sex were used. We used simplified genotypes of mouse strains for clarity.

HEK 293T cell culture

HEK 293T cells were obtained from the American Type Culture Collection (ATCC). Cells were cultured at 37°C in 5% CO_2 in DMEM supplemented with 10% (v/v) fetal bovine serum (FBS) and 1% penicillin-streptomycin. HEK 293T stable cell lines were generated using lentivirus; transduced monoclonal cells were selected to perform the experiments. Antibiotic selection was used to maintain long-term gene expression.

Primary astrocyte culture

Primary astrocyte cultures were prepared from the cerebral cortices of mouse pups (P0) as described previously (Schildge et al., 2013). Briefly, cortices were dissected free of meninges and placed in DMEM/F12 containing 1% penicillin-streptomycin and no FBS. Following mechanical dissociation and filtration with 40 μm cell sieves, the cells were collected by centrifugation (200×*g*) at room temperature for 10 min. The cells were suspended in DMEM/F12 medium of 10% FBS and 1% penicillin-streptomycin and plated in the culture flask. Cultures were grown for 14 d in a 37°C incubation chamber with 5% CO_2 with regular media changes. Following shaking on a 37°C shaker for 2 h at 180–200 r min^{-1}, we retrieved the cells left at the bottom of the flask.

DNA plasmids and viral constructs

Chicken *Opn5*, human *Opn5*, mouse *Opn5* and mouse *Opn4L* sequences were synthesized (Azenta Life Sciences, Tianjin, China). Table S1 in Supporting Information provides a detailed list of the three opsins, their species, GenBank accession numbers and the aliases used in the main text of this paper. Cell-filling versions of all the opsins were constructed using a ribosomal skip site (T2A) between the opsin and fluorescent proteins. DNA fragments were generated using PCR amplification with primers containing 20 base-pair overlap (Azenta Life Sciences) and then assembled into plasmids using Gibson assembly (Table S2 in Supporting Information). For cultured cell studies, all genes were subcloned into a lentiviral backbone pLJM1 vector (Addgene plasmid #19319) under a CMV promoter to make vector *pLJM1-Opn5*. *cOpn5* gene was subcloned into *pLJM1* vector with C-terminal V5 tag fusion and *T2A-EGFP* for bicistronic expression.

For *in vivo* neuron studies, cOpn5 gene was subcloned into pAAV vector under the human synapsin promoter (hSyn) promoter or the CaMKII promoter with T2A-EGFP bicistronic expression. cOpn5 used in astrocytes was also subcloned into a pAAV backbone, but under a GfaABC1D promoter. The Cre-dependent *cOpn5-T2A-eGFP* vector was generated using the vector with lox sites flanking the protein-coding region under *EF1a* promoter. The plasmids were amplified and then purified using Endo Free Plasmid Maxi kit (Vazyme, Nanjing, China). The *pcDNA3.1*/*opto-a1AR-EYFP* plasmids were obtained through Addgene (plasmid #20947). *CAAX-EGFP* was a gift from Yulong Li (Peking University, China). All restriction enzymes used for molecular cloning were from New England Biolabs and the constructs were verified using Sanger sequencing.

AAV vectors carrying *EF1a-DIO-cOpn5-T2A-eGFP* and *hSyn-cOpn5-T2A-eGFP* constructs were packaged into AAV2/9 serotype. GfaABC1D-cOpn5-T2A-eGFP was packaged into AAV2/8 serotype. We purchased the *AAV9-hSyn-NES-jRGECO1a-WPRE* from WZ Biosciences Inc. with titers of 1×10^{13} viral particles per milliliter. All Plasmids and Viral constructs used in this paper were listed in Table S3 in Supporting Information.

Common surgery and virus injection

Adult mice were anesthetized with avertin (i.p. 300 mg kg^{-1}) before surgery and then placed in a stereotaxic apparatus. After disinfection with 0.3% hydrogen peroxide, a small incision of the scalp was created to expose the skull. Craniotomy was conducted above the targeted brain areas using the following coordinates (mm in AP, DV, ML with respect to the bregma): −0.7, −4.75, ±1.0 for the lateral hypothalamus, −1.0, −4.4, ±0.7 for the zona incerta, 0.2, −3.5, 1.8 for the dorsal striatum, and 1.8, −1.9, 1.7 for the hippocampus. We used a microsyringe pump (Nanoliter 2010 Injector, WPI, USA) and a Micro4 controller to slowly infused AAV virus into each site (46 nL min^{-1} speed; a total volume of 100 nL unless described otherwise).

Immunohistochemistry, histology and fluorescent microscopy

For immunofluorescence, cultured HEK 293T cells transiently-transfected with pLJM1-cmv-V5-Opn5 and primary astrocytes cells were washed with PBS for three times and fixed with 4% paraformaldehyde (PFA, wt/vol in PBS) for 20 min at room temperature. The fixed cells were washed with PBS again and were then blocked with 3% FBS and 0.3% Triton X-100 for 30 min followed by staining with the

primary antibodies for 2 h at room temperature. Cells were washed with PBS for three times and stained with the secondary antibodies. Primary antibodies used were anti-V5 (mouse, Thermo Fisher Scientific, USA) and anti-GFAP (rabbit, Abcam, UK). Secondary antibodies used were Alexa Fluor 546 goat anti-mouse secondary antibody (Jackson ImmunoResearch, USA) and Cy3-AffiniPure Goat Anti-Rabbit secondary antibody (Jackson ImmunoResearch).

Fluorescent images were acquired on a Zeiss confocal microscope (LSM880, 40×, NA1.3 oil-immersion lens; Zeiss, Germany) or an Olympus VS120 virtual microscopy slide scanning system (10× objective; Olympus, Japan) and further processed using ImageJ (1.53 h).

Immunoblotting

For western blotting, cOpn5-HEK 293T cells were pretreated with 10 μmol L^{-1} staurosporine or buffer control for 60 min before irradiation with 470 nm light for 3 min (5 s on, 5 s off, 100 μW mm^{-2}). The protein samples were directly lysed into 1× SDS loading buffer immediately after the light was off. After electrophoresed by SDS-PAGE at 110 V, the separated proteins were transferred onto PVDF membranes and blocked with 5% nonfat milk in Tris-buffered with 0.1% Tween® 20 Detergent (TBST) buffer. Membranes were incubated with primary antibodies anti-Phospho-MARCKS (Cell Signaling Technology, USA) and anti-alpha-tubulin (Sigma-Aldrich, USA) in blocking buffer overnight. Membranes were washed three times in TBST before incubation in 1:30,000 species-specific HRP-conjugated antibodies (Thermo Fisher Scientific). Membranes were washed again three times in TBST before visualization with Enhanced Chemiluminescence substrate. ImageJ was used to quantify protein bands from western blot films.

cAMP and IP_1 Assay

For IP_1 assays, HEK 293T cells that stably expressed cOpn5 or hOPN5 were optically stimulated for 3 min (100 μW mm^{-2}, 470 nm) in LiCl-containing buffer, with or without 10 nmol L^{-1} YM-254890 pretreatment to block the G_q proteins. After 1 h incubation, accumulation of IP_1 was measured by a competitive immunoassay according to the manufacturer's instructions with an ELISA kit (CisBio, France).

For cAMP assays, HEK 293T cells that stably expressed chicken, mouse, human Opn5s were incubated with or without 10 μmol L^{-1} all trans-retinal 24 h in the dark, and the cells were supplied with 10 μmol L^{-1} forskolin 30 min before light stimulation with 470 nm for 3 min (5 s on, 5 s off, 100 μW mm^{-2}). The cAMP concentration in the cell lysis was measured with an ELISA kit according to the manufacturer's protocol (Wuhan Bioyeargene Biotechnology, Wuhan, China).

Ca^{2+} imaging of cell cultures

Table S4 in Supporting Information provides detailed information on light excitation sources, microscopes, and key experimental parameters.

Specifically, HEK 293T cells were transiently transfected to express Opn5s (chicken, human and mouse) and loaded with Ca^{2+} indicator Calbryte 630-AM (5 μmol L^{-1}) for 1 h in Hank's Balanced Salt Solution (HBSS) buffer. Images were captured and analyzed by Nikon confocal microscopy (A1R, 25×, NA1.1 water-immersion lens, Nikon, Japan) with the NIS-Elements software (5.20.00). For image acquisition, we used the 488 nm from microscope light source.

cOpn5-HEK 293T stable cells were loaded with Ca^{2+} indicator Calbryte 630-AM (5 μmol L^{-1}) for 1 h in HBSS. Nominal Ca^{2+}-free buffer was made by discarding the calcium in HBSS. Spinning disk confocal system was used to investigate the spectral characteristic of cOpn5. We adjusted the wavelength (365, 395, 470, 515, 561, 590, and 630 nm), duration (1, 5, 10, 20, and 50 ms; 470 nm), and intensity (0, 4.8, 8, 16, or 32 μW mm^{-2}; 470 nm; 10 ms) of optical stimulation.

We stimulated HEK 293T cells transiently expressing opto-a1AR with 515 nm light (7 mW mm^{-2}, 60 s). For mOPN4L-expressing cells, we used 470 nm light (40 mW mm^{-2}, 25 s) with or without 10 μmol L^{-1} ATR. For chemogenetic activation, we stimulated HEK 293T cells expressing hM3Dq with local puff applications of CNO (100 nmol L^{-1}) near the imaging field.

To observe the effect of spatially restricted stimulation on Ca^{2+} signals, we used Nikon A1R enabled spatially patterned illumination and a 25×, NA1.1 water-immersion lens to stimulate a small area (488 nm; 3.7 μm×3.7 μm for stimulating single cOpn5-HEK 293T cell) to determine Ca^{2+} wave propagations. The sampling rate was 2 fps at a size of 384×286 pixels.

Acquired data were analyzed by the Matlab and ImageJ software. Typically, we photostimulated and imaged 5 separate regions per well and repeated 3 wells per condition.

Behavioral tasks and *in vivo* optogenetics

Mice had *ad libitum* access to normal mouse lab pellet food and water before the tests. Mice were allowed to recover for at least two weeks following stereotaxic infusion of AAV vectors and the implant of optic fiber ferrule. On the test day, an optical fiber (200 μm diameter, 0.37 NA; Shanghai Fiblaser, China) was connected to the ferrule. *VGAT*-Cre mice expressing *cOpn5-T2A-EGFP* or *EGFP* alone were placed in the test chamber. To generate light pulses, we used a Master-8 pulse stimulator (A.M.P.I., Israel) to control the light de-

livery (473 nm; peak light power 0.75 mW) from a solid state laser (MBL-III-473, Changchun New Industries Optoelectronics Technology, China). For the food intake assay, we measured the amount of food consumed before and during optogenetic stimulation (30 min off, 30 min on using 20 Hz blue light pulses). For the food foraging test, high-fat food pellets were hidden in the bedding litter. Mouse received light stimulation until the hidden food pellet was retrieved. Foraging time was calculated since the blue light on until the mouse got the food. Mouse behaviors were videotaped via a camera 30 cm above the chamber. Pellet retrieval time was calculated by manual video scoring offline.

Electrophysiological recording and Ca^{2+} Imaging in brain slices

Slice preparation and electrophysiological recordings were performed as described previously (Zhang et al., 2016). Briefly, mice were deeply anesthetized with pentobarbital (100 mg kg^{-1} i.p.) and intracardially perfused with 5 mL ice-cold oxygenated perfusion solution containing (in mmol L^{-1}) 1.25 glucose, 225 sucrose, 119 NaCl, 2.5 KCl, 0.1 $CaCl_2$, 4.9 $MgCl_2$, 1.0 NaH_2PO_4, 26.2 $NaHCO_3$, 3 kynurenic acid, and 1 Na L-ascorbate (all chemicals for brain slicing recording were from Sigma-Aldrich). The mouse brain was rapidly removed and placed in ice-cold oxygenated slicing solution containing (in mmol L^{-1}) 110 choline chloride, 2.5 KCL, 0.5 $CaCl_2$, 7 $MgCl_2$, 1.3 NaH_2PO_4, 25 $NaHCO_3$, 20 Glucose, 1.3 Na ascorbate, and 0.6 Na pyruvate. Coronal sections (250 μm thick) were prepared with a Leica VT1200S vibratome. The slices were incubated for 1 h at 34°C with ringer solution saturated with a 95%:5% mixture of O_2:CO_2. The ringer solution consisted of (in mmol L^{-1}) 125 NaCl, 2.5 KCl, 2 $CaCl_2$, 1.3 $MgCl_2$, 1.3 NaH_2PO_4, 25 $NaHCO_3$, 10 Glucose, 1.3 Na ascorbate, and 0.6 Na pyruvate. The intrapipette solution contained (in mmol L^{-1}) 130 K-gluconate, 10 HEPES, 0.6 EGTA, 5 KCl, 3 Na_2ATP, 0.3 Na_3GTP, 4 $MgCl_2$, and 10 Na_2-phosphocreatine (pH 7.2–7.4). Whole-cell patch-clamp recordings were made on mouse brain slices using a Multiclamp 700B amplifier, which was connected to a Digidata 1440 digitizer (Molecular Devices, USA) and attached to a PC running pClamp 10. Electrophysiological data were acquired at 5 kHz and low-pass filtered at 10 kHz.

For Ca^{2+} imaging, the red fluorescent signals from Calbryte™ 630 were imaged on a two-photon microscope (Olympus BX61W1, 20×, NA1.1 water-immersion lens, 2 fps). For photostimulation, blue light pulses (470 nm) were generated with an LED.

Ca^{2+} signal analysis

The images were converted into TIF files and analyzed by CaImAnalyzer MATLAB program. Briefly, we defined each cell as an individual region of interest (ROI) and calculated the Ca^{2+} signal of the cell as $\Delta F/F=(F-F0)/F0$, where $F0$ was the average baseline fluorescence intensity within the 5 s before light or drug application, and F was the fluorescence intensity across time frames. The $\Delta F/F$ values are stored in CalData MATLAB file. We used the group_ data_plot MATLAB program to plot the signal curve of each data group.

Ca^{2+} signal propagation analysis

The images were converted into TIF files and analyzed by CellWaveforCell MATLAB program. The deltaF/F image results were obtained after running. F is the average value of the first 10 frames as the basal fluorescence value. DeltaF is the fluorescence value of each frame minus F. The results of image deltaF/F were opened with Fiji, and the pseudo-color image of fluorescence signal changing with time was obtained by image, hyperstacks and grey-color code.

Statistics

We used MATLAB 2018a and GraphPad Prism 9 to perform statistical analysis. Statistical method, the corresponding P values, and the sample sizes are reported in the figure legends as well as in Table S5 in Supporting Information. The sample sizes were not predetermined. In all optogenetic activation experiments and fiber photometry recordings, sample sizes (n) denote the number of stimulation or recording sites. In slice recording experiments, sample sizes denote the cell numbers recorded. Data were reported as mean±SEM in all Figures.

Data and code availability

Data and custom programs are available upon request. All the programs used are on the institute hosted server and can be accessed at http://imaging.cibr.ac.cn/Public/Upload/Content/20211025/617639f0637c2.rar.

Compliance and ethics *The author(s) declare that they have no conflict of interest.*

Acknowledgements *This work was supported by Ministry of Science and Technology China Brain Initiative Grant (2021ZD0202803), the Research Unit of Medical Neurobiology at Chinese Academy of Medical Sciences (2019RU003), and Beijing Municipal Government. We would like to thank members of Luo laboratory for critical discussion of the paper. We thank the Imaging cores at Chinese Institute for Brain Research, Beijing and National Institute of Biological Sciences, Beijing for technical assistance.*

References

Abbott, N.J., Rönnbäck, L., and Hansson, E. (2006). Astrocyte-endothelial

interactions at the blood-brain barrier. Nat Rev Neurosci 7, 41–53.
Adams, S.R., and Tsien, R.Y. (1993). Controlling cell chemistry with caged compounds. Annu Rev Physiol 55, 755–784.
Airan, R.D., Thompson, K.R., Fenno, L.E., Bernstein, H., and Deisseroth, K. (2009). Temporally precise *in vivo* control of intracellular signalling. Nature 458, 1025–1029.
Allen, N.J., and Eroglu, C. (2017). Cell biology of astrocyte-synapse interactions. Neuron 96, 697–708.
Bellono, N.W., Kammel, L.G., Zimmerman, A.L., and Oancea, E. (2013). UV light phototransduction activates transient receptor potential A1 ion channels in human melanocytes. Proc Natl Acad Sci USA 110, 2383–2388.
Boyden, E.S., Zhang, F., Bamberg, E., Nagel, G., and Deisseroth, K. (2005). Millisecond-timescale, genetically targeted optical control of neural activity. Nat Neurosci 8, 1263–1268.
Brueggemann, L.I., and Sullivan, J.M. (2002). HEK293S cells have functional retinoid processing machinery. J Gen Physiol 119, 593–612.
Calligaro, H., Dkhissi-Benyahya, O., and Panda, S. (2022). Ocular and extraocular roles of neuropsin in vertebrates. Trends Neuroscis 45, 200–211.
Clapham, D.E. (2007). Calcium signaling. Cell 131, 1047–1058.
Copits, B.A., Gowrishankar, R., O'Neill, P.R., Li, J.N., Girven, K.S., Yoo, J.J., Meshik, X., Parker, K.E., Spangler, S.M., Elerding, A.J., et al. (2021). A photoswitchable GPCR-based opsin for presynaptic inhibition. Neuron 109, 1791–1809.e11.
Dai, R., Yu, T., Weng, D., Li, H., Cui, Y., Wu, Z., Guo, Q., Zou, H., Wu, W., Gao, X., et al. (2022). A neuropsin-based optogenetic tool for precise control of G_q signaling. bioRxiv 2022.02.22.481462.
Exton, J.H. (1996). Regulation of phosphoinositide phospholipases by hormones, neurotransmitters, and other agonists linked to G proteins. Annu Rev Pharmacol Toxicol 36, 481–509.
Fenno, L., Yizhar, O., and Deisseroth, K. (2011). The development and application of optogenetics. Annu Rev Neurosci 34, 389–412.
Figueiredo, M., Lane, S., Stout Jr., R.F., Liu, B., Parpura, V., Teschemacher, A.G., and Kasparov, S. (2014). Comparative analysis of optogenetic actuators in cultured astrocytes. Cell Calcium 56, 208–214.
Gerasimov, E., Erofeev, A., Borodinova, A., Bolshakova, A., Balaban, P., Bezprozvanny, I., and Vlasova, O.L. (2021). Optogenetic activation of astrocytes—effects on neuronal network function. Int J Mol Sci 22, 9613.
Gomez, J.L., Bonaventura, J., Lesniak, W., Mathews, W.B., Sysa-Shah, P., Rodriguez, L.A., Ellis, R.J., Richie, C.T., Harvey, B.K., Dannals, R.F., et al. (2017). Chemogenetics revealed: DREADD occupancy and activation via converted clozapine. Science 357, 503–507.
Güler, A.D., Ecker, J.L., Lall, G.S., Haq, S., Altimus, C.M., Liao, H.W., Barnard, A.R., Cahill, H., Badea, T.C., Zhao, H., et al. (2008). Melanopsin cells are the principal conduits for rod-cone input to non-image-forming vision. Nature 453, 102–105.
Hankins, M.W., Peirson, S.N., and Foster, R.G. (2008). Melanopsin: an exciting photopigment. Trends Neuroscis 31, 27–36.
Hartwig, J.H., Thelen, M., Rosen, A., Janmey, P.A., Nairn, A.C., and Aderem, A. (1992). MARCKS is an actin filament crosslinking protein regulated by protein kinase C and calcium-calmodulin. Nature 356, 618–622.
Hattar, S., Liao, H.W., Takao, M., Berson, D.M., and Yau, K.W. (2002). Melanopsin-containing retinal ganglion cells: architecture, projections, and intrinsic photosensitivity. Science 295, 1065–1070.
Hauser, A.S., Attwood, M.M., Rask-Andersen, M., Schiöth, H.B., and Gloriam, D.E. (2017). Trends in GPCR drug discovery: new agents, targets and indications. Nat Rev Drug Discov 16, 829–842.
Herlitze, S., and Landmesser, L.T. (2007). New optical tools for controlling neuronal activity. Curr Opin Neurobiol 17, 87–94.
Hu, Q.M., Yi, W.J., Su, M.Y., Jiang, S., Xu, S.Z., and Lei, T.C. (2017). Induction of retinal-dependent calcium influx in human melanocytes by UVA or UVB radiation contributes to the stimulation of melanosome transfer. Cell Prolif 50, e12372.
Jennings, J.H., Rizzi, G., Stamatakis, A.M., Ung, R.L., and Stuber, G.D. (2013). The inhibitory circuit architecture of the lateral hypothalamus orchestrates feeding. Science 341, 1517–1521.
Kadamur, G., and Ross, E.M. (2013). Mammalian phospholipase C. Annu Rev Physiol 75, 127–154.
Kojima, D., Mori, S., Torii, M., Wada, A., Morishita, R., and Fukada, Y. (2011). UV-sensitive photoreceptor protein OPN5 in humans and mice. PLoS ONE 6, e26388.
Koyanagi, M., and Terakita, A. (2014). Diversity of animal opsin-based pigments and their optogenetic potential. Biochim Biophys Acta 1837, 710–716.
Krashes, M.J., Koda, S., Ye, C.P., Rogan, S.C., Adams, A.C., Cusher, D.S., Maratos-Flier, E., Roth, B.L., and Lowell, B.B. (2011). Rapid, reversible activation of AgRP neurons drives feeding behavior in mice. J Clin Invest 121, 1424–1428.
Li, Y., Zeng, J., Zhang, J., Yue, C., Zhong, W., Liu, Z., Feng, Q., and Luo, M. (2018). Hypothalamic circuits for predation and evasion. Neuron 97, 911–924.e5.
Lin, J.Y. (2011). A user's guide to channelrhodopsin variants: features, limitations and future developments. Exp Physiol 96, 19–25.
Linnerbauer, M., Wheeler, M.A., and Quintana, F.J. (2020). Astrocyte crosstalk in CNS inflammation. Neuron 108, 608–622.
Lu, L., Wang, R., and Luo, M. (2020). An optical brain-to-brain interface supports rapid information transmission for precise locomotion control. Sci China Life Sci 63, 875–885.
Luo, Q. (2020). A brief introduction to biophotonic techniques and methods. Sci China Life Sci 63, 1771–1775.
Mahn, M., Saraf-Sinik, I., Patil, P., Pulin, M., Bitton, E., Karalis, N., Bruentgens, F., Palgi, S., Gat, A., Dine, J., et al. (2021). Efficient optogenetic silencing of neurotransmitter release with a mosquito rhodopsin. Neuron 109, 1621–1635.e8.
Mederos, S., Hernández-Vivanco, A., Ramírez-Franco, J., Martín-Fernández, M., Navarrete, M., Yang, A., Boyden, E.S., and Perea, G. (2019). Melanopsin for precise optogenetic activation of astrocyte-neuron networks. Glia 67, 915–934.
Melyan, Z., Tarttelin, E.E., Bellingham, J., Lucas, R.J., and Hankins, M.W. (2005). Addition of human melanopsin renders mammalian cells photoresponsive. Nature 433, 741–745.
Mure, L.S., Hatori, M., Zhu, Q., Demas, J., Kim, I.M., Nayak, S.K., and Panda, S. (2016). Melanopsin-encoded response properties of intrinsically photosensitive retinal ganglion cells. Neuron 90, 1016–1027.
Nakane, Y., Ikegami, K., Ono, H., Yamamoto, N., Yoshida, S., Hirunagi, K., Ebihara, S., Kubo, Y., and Yoshimura, T. (2010). A mammalian neural tissue opsin (Opsin 5) is a deep brain photoreceptor in birds. Proc Natl Acad Sci USA 107, 15264–15268.
Nakane, Y., Shimmura, T., Abe, H., and Yoshimura, T. (2014). Intrinsic photosensitivity of a deep brain photoreceptor. Curr Biol 24, R596–R597.
Panda, S., Provencio, I., Tu, D.C., Pires, S.S., Rollag, M.D., Castrucci, A.M., Pletcher, M.T., Sato, T.K., Wiltshire, T., Andahazy, M., et al. (2003). Melanopsin is required for non-image-forming photic responses in blind mice. Science 301, 525–527.
Panda, S., Nayak, S.K., Campo, B., Walker, J.R., Hogenesch, J.B., and Jegla, T. (2005). Illumination of the melanopsin signaling pathway. Science 307, 600–604.
Qiu, X., Kumbalasiri, T., Carlson, S.M., Wong, K.Y., Krishna, V., Provencio, I., and Berson, D.M. (2005). Induction of photosensitivity by heterologous expression of melanopsin. Nature 433, 745–749.
Quadrato, G., Nguyen, T., Macosko, E.Z., Sherwood, J.L., Min Yang, S., Berger, D.R., Maria, N., Scholvin, J., Goldman, M., Kinney, J.P., et al. (2017). Cell diversity and network dynamics in photosensitive human brain organoids. Nature 545, 48–53.
Rios, M.N., Marchese, N.A., and Guido, M.E. (2019). Expression of non-visual opsins Opn3 and Opn5 in the developing inner retinal cells of birds. Light-responses in Müller glial cells. Front Cell Neurosci 13, 376.
Ritter, S.L., and Hall, R.A. (2009). Fine-tuning of GPCR activity by receptor-interacting proteins. Nat Rev Mol Cell Biol 10, 819–830.

Rogan, S.C., and Roth, B.L. (2011). Remote control of neuronal signaling. Pharmacol Rev 63, 291–315.
Rosenbaum, D.M., Rasmussen, S.G.F., and Kobilka, B.K. (2009). The structure and function of G-protein-coupled receptors. Nature 459, 356–363.
Rost, B.R., Schneider-Warme, F., Schmitz, D., and Hegemann, P. (2017). Optogenetic tools for subcellular applications in neuroscience. Neuron 96, 572–603.
Roth, B.L. (2016). DREADDs for neuroscientists. Neuron 89, 683–694.
Schildge, S., Bohrer, C., Beck, K., and Schachtrup, C. (2013). Isolation and culture of mouse cortical astrocytes. J Vis Exp doi: 10.3791/50079.
Sofroniew, M.V. (2015). Astrocyte barriers to neurotoxic inflammation. Nat Rev Neurosci 16, 249–263.
Spoida, K., Masseck, O.A., Deneris, E.S., and Herlitze, S. (2014). Gq/5-HT_{2c} receptor signals activate a local GABAergic inhibitory feedback circuit to modulate serotonergic firing and anxiety in mice. Proc Natl Acad Sci USA 111, 6479–6484.
Spoida, K., Eickelbeck, D., Karapinar, R., Eckhardt, T., Mark, M.D., Jancke, D., Ehinger, B.V., König, P., Dalkara, D., Herlitze, S., et al. (2016). Melanopsin variants as intrinsic optogenetic on and off switches for transient versus sustained activation of G protein pathways. Curr Biol 26, 1206–1212.
Stuber, G.D., and Wise, R.A. (2016). Lateral hypothalamic circuits for feeding and reward. Nat Neurosci 19, 198–205.
Taniguchi, M., Suzumura, K., Nagai, K., Kawasaki, T., Saito, T., Takasaki, J., Suzuki, K., Fujita, S., and Tsukamoto, S. (2003). Structure of YM-254890, a novel $G_{q/11}$ inhibitor from *Chromobacterium* sp. QS3666. Tetrahedron 59, 4533–4538.
Terakita, A. (2005). The opsins. Genome Biol 6, 213.
Tian, L., Hires, S.A., Mao, T., Huber, D., Chiappe, M.E., Chalasani, S.H., Petreanu, L., Akerboom, J., McKinney, S.A., Schreiter, E.R., et al. (2009). Imaging neural activity in worms, flies and mice with improved GCaMP calcium indicators. Nat Methods 6, 875–881.
Tsukamoto, H., and Terakita, A. (2010). Diversity and functional properties of bistable pigments. Photochem Photobiol Sci 9, 1435.
Tye, K.M., and Deisseroth, K. (2012). Optogenetic investigation of neural circuits underlying brain disease in animal models. Nat Rev Neurosci 13, 251–266.
Urban, D.J., and Roth, B.L. (2015). DREADDs (designer receptors exclusively activated by designer drugs): chemogenetic tools with therapeutic utility. Annu Rev Pharmacol Toxicol 55, 399–417.
Vaezy, S., Shi, X., Martin, R.W., Chi, E., Nelson, P.I., Bailey, M.R., and Crum, L.A. (2001). Real-time visualization of high-intensity focused ultrasound treatment using ultrasound imaging. Ultrasound Med Biol 27, 33–42.
Wagdi, A., Malan, D., Sathyanarayanan, U., Beauchamp, J.S., Vogt, M., Zipf, D., Beiert, T., Mansuroglu, B., Dusend, V., Meininghaus, M., et al. (2022). Selective optogenetic control of G_q signaling using human neuropsin. Nat Commun 13, 1–8.
Wettschureck, N., and Offermanns, S. (2005). Mammalian G proteins and their cell type specific functions. Physiol Rev 85, 1159–1204.
Xie, A.X., Petravicz, J., and McCarthy, K.D. (2015). Molecular approaches for manipulating astrocytic signaling *in vivo*. Front Cell Neurosci 9, 144.
Xue, T., Do, M.T.H., Riccio, A., Jiang, Z., Hsieh, J., Wang, H.C., Merbs, S. L., Welsbie, D.S., Yoshioka, T., Weissgerber, P., et al. (2011). Melanopsin signalling in mammalian iris and retina. Nature 479, 67–73.
Yamashita, T., Ohuchi, H., Tomonari, S., Ikeda, K., Sakai, K., and Shichida, Y. (2010). Opn5 is a UV-sensitive bistable pigment that couples with Gi subtype of G protein. Proc Natl Acad Sci USA 107, 22084–22089.
Yau, K.W., and Hardie, R.C. (2009). Phototransduction motifs and variations. Cell 139, 246–264.
Yu, X., Nagai, J., and Khakh, B.S. (2020). Improved tools to study astrocytes. Nat Rev Neurosci 21, 121–138.
Zhang, F., Wang, L.P., Boyden, E.S., and Deisseroth, K. (2006). Channelrhodopsin-2 and optical control of excitable cells. Nat Methods 3, 785–792.
Zhang, F., Vierock, J., Yizhar, O., Fenno, L.E., Tsunoda, S., Kianianmomeni, A., Prigge, M., Berndt, A., Cushman, J., Polle, J., et al. (2011). The microbial opsin family of optogenetic tools. Cell 147, 1446–1457.
Zhang, J., Tan, L., Ren, Y., Liang, J., Lin, R., Feng, Q., Zhou, J., Hu, F., Ren, J., Wei, C., et al. (2016). Presynaptic excitation via GABAB receptors in habenula cholinergic neurons regulates fear memory expression. Cell 166, 716–728.
Zhang, K.X., D'Souza, S., Upton, B.A., Kernodle, S., Vemaraju, S., Nayak, G., Gaitonde, K.D., Holt, A.L., Linne, C.D., Smith, A.N., et al. (2020). Violet-light suppression of thermogenesis by opsin 5 hypothalamic neurons. Nature 585, 420–425.
Zhang, X., and van den Pol, A.N. (2017). Rapid binge-like eating and body weight gain driven by zona incerta GABA neuron activation. Science 356, 853–859.
Zonta, M., Angulo, M.C., Gobbo, S., Rosengarten, B., Hossmann, K.A., Pozzan, T., and Carmignoto, G. (2003). Neuron-to-astrocyte signaling is central to the dynamic control of brain microcirculation. Nat Neurosci 6, 43–50.

SUPPORTING INFORMATION

The supporting information is available online at https://doi.org/10.1007/s11427-022-2122-0. The supporting materials are published as submitted, without typesetting or editing. The responsibility for scientific accuracy and content remains entirely with the authors.